

AD-A063 820

RAYTHEON CO BEDFORD MASS MISSILE SYSTEMS DIV  
DUAL FREQUENCY ARRAY TECHNIQUES EXPERIMENTAL STUDY. (U)  
AUG 78 J H POZGAY

F/G 9/5

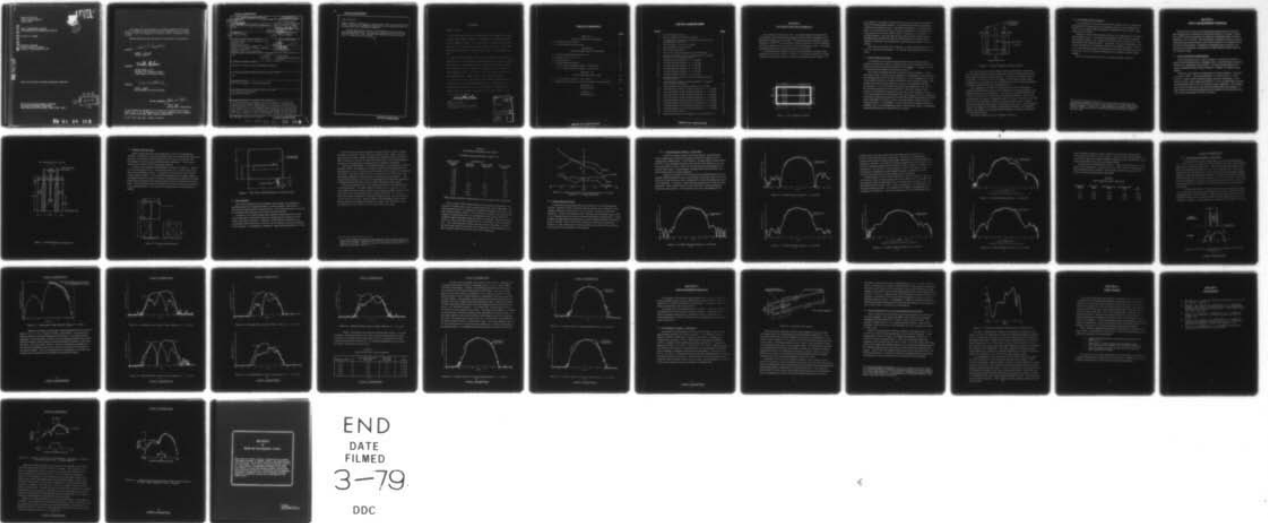
UNCLASSIFIED

BR-10222

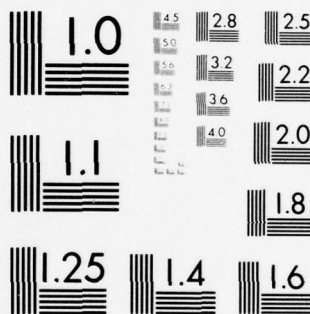
RADC-TR-78-178

F19628-77-C-0112  
NL

1 OF 1  
AD  
A063 820



END  
DATE  
FILMED  
3-79  
DDC



MICROCOPY RESOLUTION TEST CHART  
 NATIONAL BUREAU OF STANDARDS-1963-A

RADC-TR-78-178  
Final Technical Report  
August 1978



**LEVEL #**

**AD A063820**

DUAL FREQUENCY ARRAY  
TECHNIQUES EXPERIMENTAL STUDY

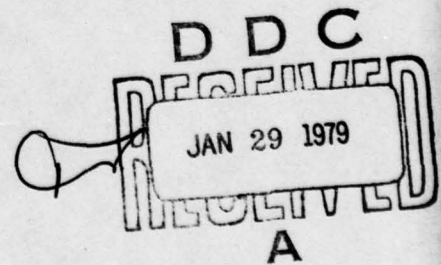
Jerome H. Pozgay

Raytheon Company  
Missile Systems Division  
Bedford, Massachusetts 01730

**DDC FILE COPY.**

Approved for public release; distribution unlimited.

ROME AIR DEVELOPMENT CENTER  
AIR FORCE SYSTEMS COMMAND  
GRIFFISS AIR FORCE BASE, NEW YORK 13441

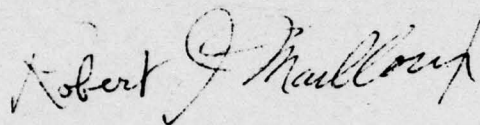


**79 01 26 013**

This report has been reviewed by the RADC Information Office (OI) and is releasable to the National Technical Information Service (NTIS). At NTIS it will be releasable to the general public, including foreign nations.

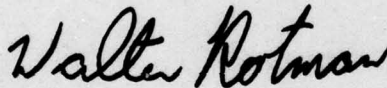
RADC-TR-78-178 has been reviewed and is approved for publication.

APPROVED:



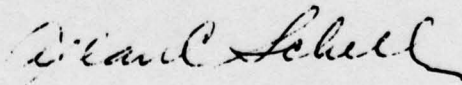
ROBERT J. MAILLOUX  
Contract Monitor

APPROVED:



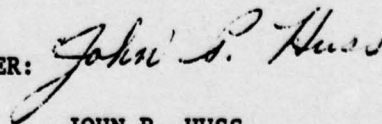
WALTER ROTMAN, Chief  
Antennas & RF Components Branch  
Electromagnetic Sciences Division

APPROVED:



ALLAN C. SCHELL  
Electromagnetic Sciences Division

FOR THE COMMANDER:



JOHN P. HUSS  
Acting Chief, Plans Office

If your address has changed or if you wish to be removed from the RADC mailing list, or if the addressee is no longer employed by your organization, please notify RADC (EEA), Hanscom AFB MA 01730.

Do not return this copy. Retain or destroy.



UNCLASSIFIED

19 REPORT DOCUMENTATION PAGE		READ INSTRUCTIONS BEFORE COMPLETING FORM
18 1. REPORT NUMBER RADC-TR-78-178	2. GOVT ACCESSION NO.	3. RECIPIENT'S CATALOG NUMBER Final Technical Report.
6 4. TITLE (and Subtitle) DUAL FREQUENCY ARRAY TECHNIQUES EXPERIMENTAL STUDY.	9	5. TYPE OF REPORT & PERIOD COVERED Final Technical Report, Feb 77 - Jan 78
	14	6. PERFORMING ORG. REPORT NUMBER BR-10222
10 7. AUTHOR(s) Jerome H. Pozgay	15	8. CONTRACT OR GRANT NUMBER(s) F19628-77-C-0112
9. PERFORMING ORGANIZATION NAME AND ADDRESS Raytheon Company, Missile Systems Division Hartwell Road Bedford MA 01730	16	10. PROGRAM ELEMENT, PROJECT, TASK AREA & WORK UNIT NUMBERS 62702F 46001430
11. CONTROLLING OFFICE NAME AND ADDRESS Deputy for Electronic Technology (RADC/EEA) Hanscom AFB MA 01730 Monitor/Robert J. Mailloux/EEA	11	12. REPORT DATE August 1978
14. MONITORING AGENCY NAME & ADDRESS (if different from Controlling Office) Same	12 44 p.	13. NUMBER OF PAGES 46
		15. SECURITY CLASS. (of this report) UNCLASSIFIED
		15a. DECLASSIFICATION/DOWNGRADING SCHEDULE N/A
16. DISTRIBUTION STATEMENT (of this Report)  Approved for public release; distribution unlimited.		
17. DISTRIBUTION STATEMENT (of the abstract entered in Block 20, if different from Report)  Same		
18. SUPPLEMENTARY NOTES RADC Project Engineer: Robert Mailloux (EEA)		
19. KEY WORDS (Continue on reverse side if necessary and identify by block number) Dual Frequency Array Element Coax-Fed Notch Exciter		
20. ABSTRACT (Continue on reverse side if necessary and identify by block number) An experimental investigation of the twin slab dual frequency array element and low frequency element exciter is presented. Principal plane radiation patterns of the center element of a 23 element array are presented. It is shown that in the low frequency operating bands (4 GHz), the principal plane element patterns are synonymous with realized gain patterns reported previously. However, in the high frequency band (8 GHz), neither individual phase center patterns nor fully excited element patterns bear the (Cont'd)		

UNCLASSIFIED

297 620 79 01 26 018

mtj

## UNCLASSIFIED

### Item 20 (Cont'd)

normal relation to realized gain. In particular, array scan characteristics must be constructed by summing individual phase center patterns without the standard array factor exponential weighting.

A novel coax-fed notch exciter for low frequency band operation has been developed empirically. The exciter provides greater than 20 dB band isolation over most of the 16 percent band centered at 8 GHz, and better than 1.9:1 VSWR over the 4 GHz band.

UNCLASSIFIED

EVALUATION

F19628-77-C-0112

1. This Final Report describes an experimental investigation of a dual frequency array geometry operating at 4 and 8 GHz, and developed under Contract F19628-75-C-0197. This investigation included the design and construction of a twenty-three element array of dielectric slab loaded waveguides, measurement of element patterns and isolation between elements.
2. Each of the basic elements consists of a waveguide with dimensions appropriate to a 4 GHz radiator, bifurcated by a metal plate with surface perpendicular to the dominant fields to form two half-height waveguides. Each element also has four dielectric slabs which serve to guide the high frequency fields. The element is excited in-phase at the low frequency and with four separate exciters at the high frequency.
3. The results of this experimental study indicate good correlation between theoretical and experimental patterns. In addition, they demonstrate the practical utility of the concept for combining two arrays, each with separate feeds and a different pointing direction, into the same array aperture.

*Robert J. Mailloux*

ROBERT J. MAILLOUX  
Contract Monitor  
Antennas & RF Components Branch  
Electromagnetic Sciences Division

ACCESSION FOR	
NTIS	White Section <input checked="" type="checkbox"/>
DDP	Diff Section <input type="checkbox"/>
UNANNOUNCED	<input type="checkbox"/>
IDENTIFICATION	
BY	
DISTRIBUTION/AVAILABILITY CODES	
Dist.	AVAIL. AND/OR SERIAL
A	

# TABLE OF CONTENTS

	<u>Page</u>
SECTION I	
INTRODUCTION AND SUMMARY	
	1
1.1 Exciter Design Program . . . . .	2
1.2 Array Measurement Program . . . . .	4
SECTION II	
ARRAY MEASUREMENT PROGRAM	
	5
2.1 Array and Element Configurations . . . . .	5
2.2 Antenna Test Facilities . . . . .	9
2.3 Band Isolation . . . . .	10
2.4 Central Element Pattern . . . . .	13
2.4.1 Central Element Pattern - 4 GHz Band . . . . .	14
2.4.2 Central Element Pattern - 8 GHz Band . . . . .	19
SECTION III	
EXCITER DESIGN PROGRAM	
	28
3.1 Low Frequency Exciter - Description . . . . .	28
3.2 Exciter Performance in Load Terminated Twin Slab Guide . . . . .	30
SECTION IV	
CONCLUSIONS	
	32
SECTION V	
REFERENCES	
	33



## LIST OF ILLUSTRATIONS

<u>Figure</u>		<u>Page</u>
1	Dual Frequency Element . . . . .	1
2	Exciter-Feedguide Interface Concept . . . . .	3
3	23 Element Dual Frequency Demonstration Array and Developmental Exciters . . . . .	6
4	Element Aperture and Grid Design . . . . .	7
5	Element/Exciter Configuration . . . . .	8
6	Array Mounting Fixture . . . . .	9
7	Plan View of Mounting Fixture on EL/AZ Mount . . . . .	10
8	Measured Isolation at Low Frequency Port - H-Plane Incidence - 12° Sampling Interval . . . . .	13
9	H-Plane Element Pattern, F = 3.68 GHz . . . . .	14
10	H-Plane Element Pattern, F = 4.00 GHz . . . . .	15
11	H-Plane Element Pattern, F = 4.32 GHz . . . . .	15
12	E-Plane Element Pattern, F = 3.68 GHz . . . . .	16
13	E-Plane Element Pattern, F = 4.00 GHz . . . . .	17
14	E-Plane Element Pattern, F = 4.32 GHz . . . . .	17
15	Schematic Representation of Individual Phase Center H-Plane Pattern . . . . .	19
16	Individual Phase Center H-Plane Patterns - Isolated Dual Frequency Element . . . . .	20
17	Constructed H-Plane Element Pattern, F = 8 GHz . . . . .	22
18	Individual Phase Center H-Plane Patterns, F = 7.36 GHz . . . . .	23
19	Individual Phase Center H-Plane Patterns, F = 7.60 GHz . . . . .	23
20	Individual Phase Center H-Plane Patterns, F = 8.00 GHz . . . . .	24
21	Individual Phase Center H-Plane Patterns, F = 8.40 GHz . . . . .	24
22	Individual Phase Center H-Plane Patterns, F = 8.64 GHz . . . . .	25
23	E-Plane Pattern of Fully Excited Element, F = 7.36 GHz . . . . .	26
24	E-Plane Pattern of Fully Excited Element, F = 8.00 GHz . . . . .	27
25	E-Plane Pattern of Fully Excited Element, F = 8.64 GHz . . . . .	27
26	Coax Fed Notch Exciter. . . . .	29
27	Reflection Coefficient Magnitude for Coax Fed Exciter . . . . .	31



## SECTION I INTRODUCTION AND SUMMARY

The objectives of this study were: to experimentally demonstrate the performance of the bifurcated twin dielectric slab loaded rectangular waveguide dual frequency array element <sup>(1)</sup> designed and analyzed under contract F19628-75-C-0197<sup>(2)</sup>; and to develop a matched exciter for the low frequency band which exhibits natural rejection in the high frequency band. The design operating bands are 15 percent centered at 4 and 8 GHz.

The bifurcated twin dielectric slab loaded rectangular waveguide dual frequency array element shown in Figure 1 is a unique concept for providing simultaneous aperture usage at two widely separated frequency bands. At

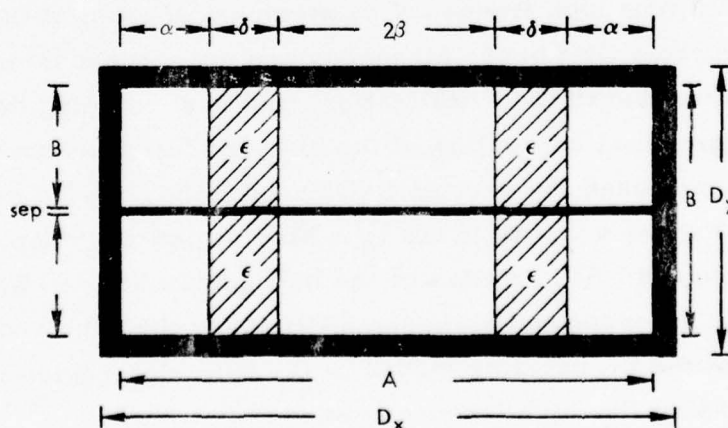


Figure 1 - Dual Frequency Element  
1

low frequency, both upper and lower halves of the waveguide are excited in-phase with equiamplitude signals. For moderate slab loading (assuming relatively thin slabs) this array will behave similarly to a rectangular waveguide array excited in the  $TE_{10}$  mode with scan behavior associated with these elements in the basic lattice (either rectangular or triangular). At the high frequency, the first odd and even half-waveguide modes can be independently specified such that four phase centers are defined; within a single low frequency cell the fields are confined predominately to the slab regions.

The study was divided into two phases: an exciter design program; and an array measurement program. The results of the phases are summarized below.

### 1.1 Exciter Design Program

The objective of the exciter design program was to develop a mode launcher for the dual frequency element which is well matched in the 4 GHz band and provides natural band isolation at the element. An exciter for the 8 GHz band was developed in the previous effort.<sup>(2)</sup>

The exciter-feedguide interface concept is shown in Figure 2. A low frequency exciter is located in the midplane of the feedguide, forward (toward the radiating aperture) of the slab terminations, and is metalized over most of its length to provide an H-plane bifurcation in the rearward regions. Two stripline-fed notch type high frequency exciters are located at the slab terminations. In the 4 GHz band, all modes are evanescent to the rear of the centered exciter due to the metalization, and port coupling decays linearly with longitudinal separation of the high and low frequency exciters. In the high frequency band the excited  $LSE_{10}$  and  $LSE_{20}$  modes are propagating with nearly equal phase velocity in the twin slab region and couple with nearly equal magnitude to the  $LSE_{10}$  modes of the half guides created by the low frequency exciter. Consequently, in the 8 GHz band the required excitation amplitude ratio of the propagating modes in the twin slab region is obtained by appropriately phasing the high frequency exciters.

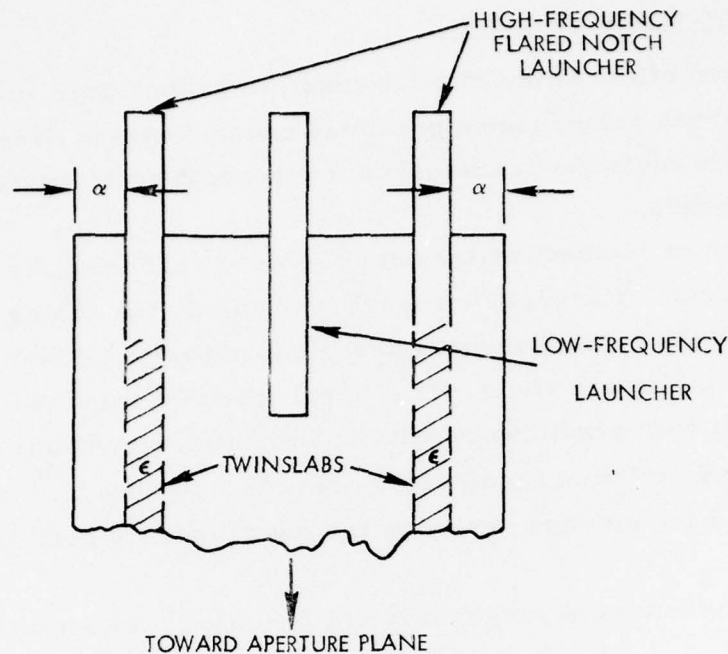


Figure 2 - Exciter-Feedguide Interface Concept

The need for natural band isolation at the element follows, primarily, from the requirement that the low frequency exciter minimally perturbs the high frequency aperture field distribution. Since the low frequency exciter is centered, it can couple only to the  $LSE_{10}$  mode of the twin slab region. Consequently, any coupling to the centered exciter in the 8 GHz band impairs scanning, grating lobe control, and element gain.

A low frequency coax-fed notch type exciter has been developed by empirical methods which achieves the objectives of the design program over limited portions of the design bands. The exciter is matched to better than 2:1 from 3.68 GHz to 4.32 GHz in load terminated feedguide. In the same configuration, the exciter mismatch exceeds 19:1 from 7.68 GHz to 7.86 GHz. Above 7.86 GHz the exciter exhibits a narrow passband which, in effect, limits the achievable high frequency bandwidth of the array. In principle this last does not appear to represent a fundamental limitation of the coax-fed exciter, but reflects an incomplete understanding of the device in the sense of an analytical model.

The exciter design program is detailed in Section 3.

## 1.2 Array Measurement Program

The objectives of the array measurement program were: to experimentally verify the array performance predicted under contract F19628-75-C-0197<sup>(2)</sup>; and to demonstrate simultaneous independent beam formation capability in the two bands.

Extensive center element pattern studies were conducted for a 23 element dual frequency array. For these measurements, only the center element was provided with the mode launchers described above; all others were load terminated at the dielectric slabs. In general, the measured patterns were in good agreement with predicted results in both frequency bands. Furthermore, natural band isolation exceeding 20 dB was demonstrated in both bands for the top\* half of the element verifying the low frequency exciter design concept.

The array measurement program is discussed fully in Section 2.

---

\*To establish feedguide reference, the element halves separated by the septum are referred to as top or bottom regardless of actual measurement plane orientation. Furthermore, high frequency ports will be referred to as left or right top (bottom) as seen looking along the outward normal to the array face.



## SECTION II

### ARRAY MEASUREMENT PROGRAM

The objectives of the array measurement program were to verify the dual frequency array performance predicted previously by Pozgay, Fassett, and Lewis<sup>(2)</sup> and to demonstrate simultaneous independent beam formation capability in the two bands. The investigation consisted primarily of central element pattern measurements in both E and H plane for a 23 element array. For these measurements, simultaneous independent beam formation was inferred under conditions of significant (>20 dB) isolation between high and low frequency feeds.

#### 2.1 Array and Element Configurations

The demonstration array, shown in Figure 3, consists of 23 dual frequency elements disposed on a triangular grid. In the 4 GHz band, the array possesses 23 independent phase centers. At high frequency there are 92 "quasi"-independent phase centers located at, roughly, the dielectric slab centers.

The basic array aperture configuration is shown in Figure 4. The grid is 1.500 x 0.960 in. The element aperture is 1.376 x 0.832 in., with a 0.032 in. E-plane septum separating upper and lower frequencies. Four dielectric slabs, with relative permittivity  $\epsilon = 5$ , are symmetrically disposed in the feedguides with 0.750 in. on center H-plane separation. This configuration has been selected for both electrical performance and simplicity of high frequency feed design (predicated on the design of a fully excited array). The array ground plane is 13.500 x 10.800 in.



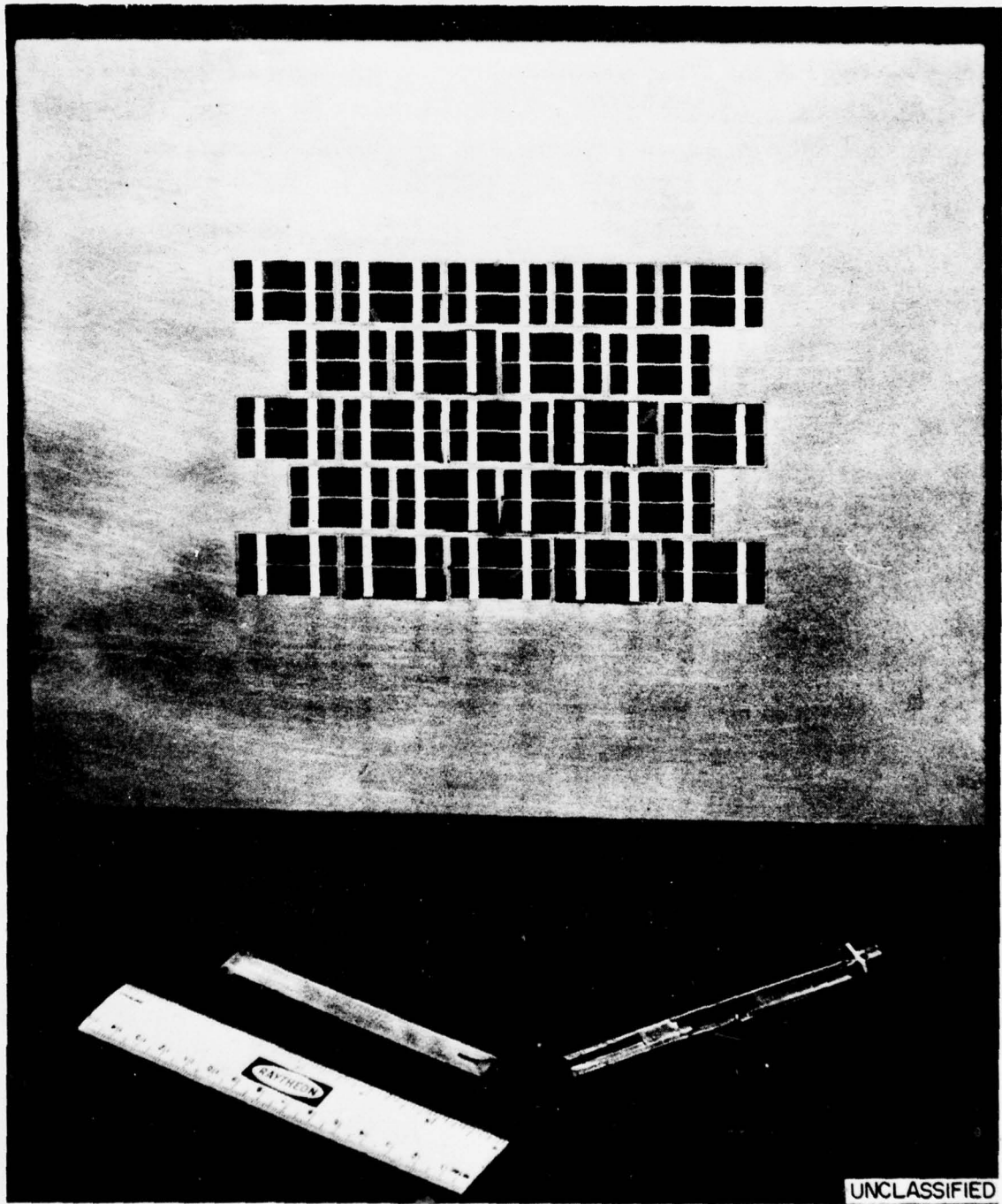
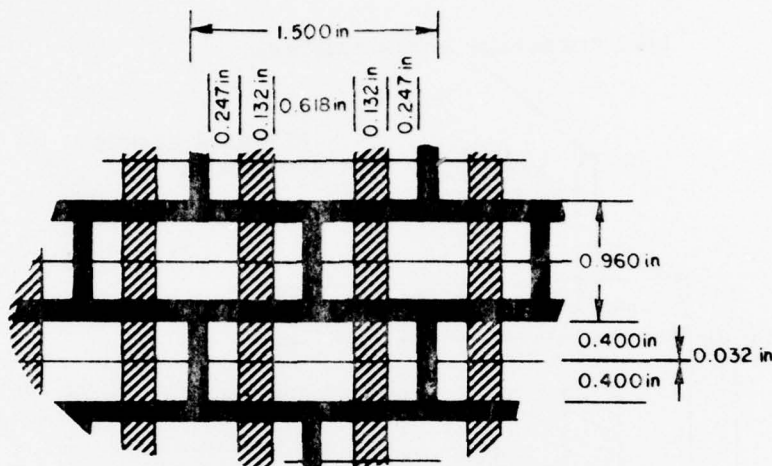


Figure 3 - 23 Element Dual Frequency Demonstration Array and <sup>778-0107</sup> Developmental Exciters



NOTE: NOT DRAWN TO SCALE

Figure 4 - Element Aperture and Grid Design

For the array measurement program, only the center element is excited; the remaining elements are load-terminated at the slab discontinuities. The loading is a tapered-free space absorber backed by a reflective surface at the element backplane and provides greater than 15 dB reflection loss.

The half-element configuration is shown in Figure 5. The total element length is 3.200 in. The low frequency exciter is 2.255 in. long and is inserted from the backplane of the element, with the coaxial probe parallel to the dielectric slabs and lying in the element midplane. Two stripline-fed tapered notch exciters<sup>(2)</sup>, similar to the stripline-fed notch antenna<sup>(3-5)</sup>, are symmetrically located about the midplane of the dielectric slabs and form the slab terminations. The longitudinal separation between the low frequency coaxial probe and the stripline-fed exciters is 0.439 in.

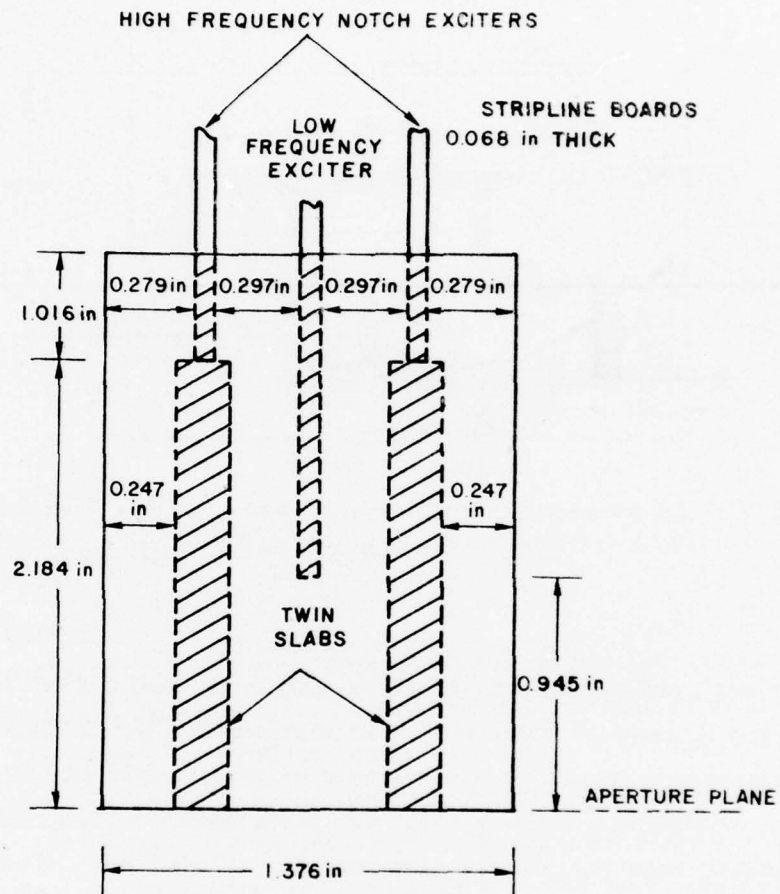


Figure 5 - Element/Exciter Configuration

## 2.2 Antenna Test Facilities

Antenna measurements were performed in a 26 ft C-band anechoic chamber, with EL/AZ mount and equipped with: an SA Series 1600 Wide Band Receiver; an SA Series 4100 Positioner Control Unit; an SA Series 1520 Rectangular Recorder; and an HP8690B Sweep Oscillator. The transmit source was an ESL 2-18 GHz dual-polarized horn.

A sketch of the antenna mounting fixture is shown in Figure 6. The fixture is constructed of 3/8 in. plywood and allows 90° rotation of the array about the ground plane normal. The position of the antenna on the EL/AZ mount, shown in Figure 7, was selected such that the array phase center is coincident with the AZ center of rotation in anticipation of anomalous H-plane pattern nulls associated with individual phase center excitation in the 8 GHz band. This positioning resulted in pattern asymmetries due to the protrusion of the elevation gear 3.5 in. forward of the table and to the broad patterns studied.

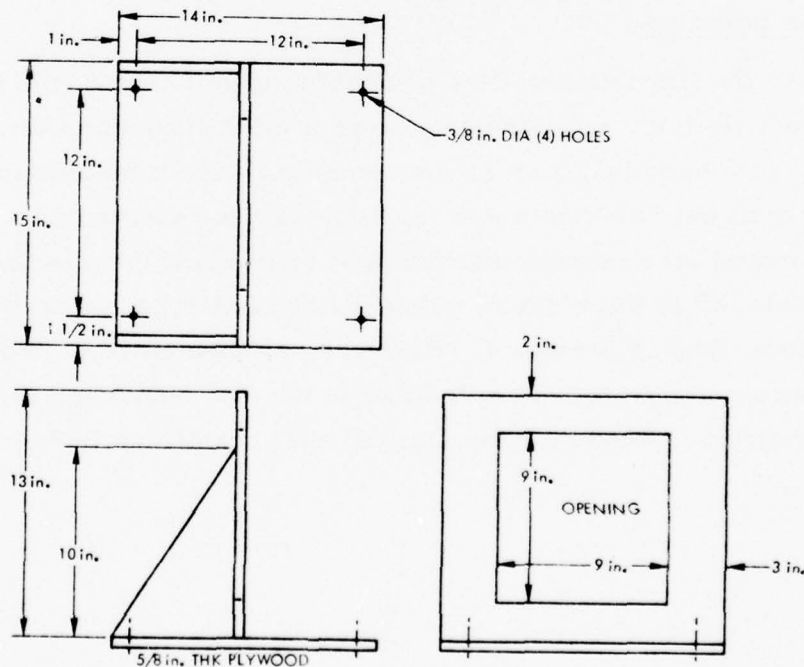


Figure 6 - Array Mounting Fixture

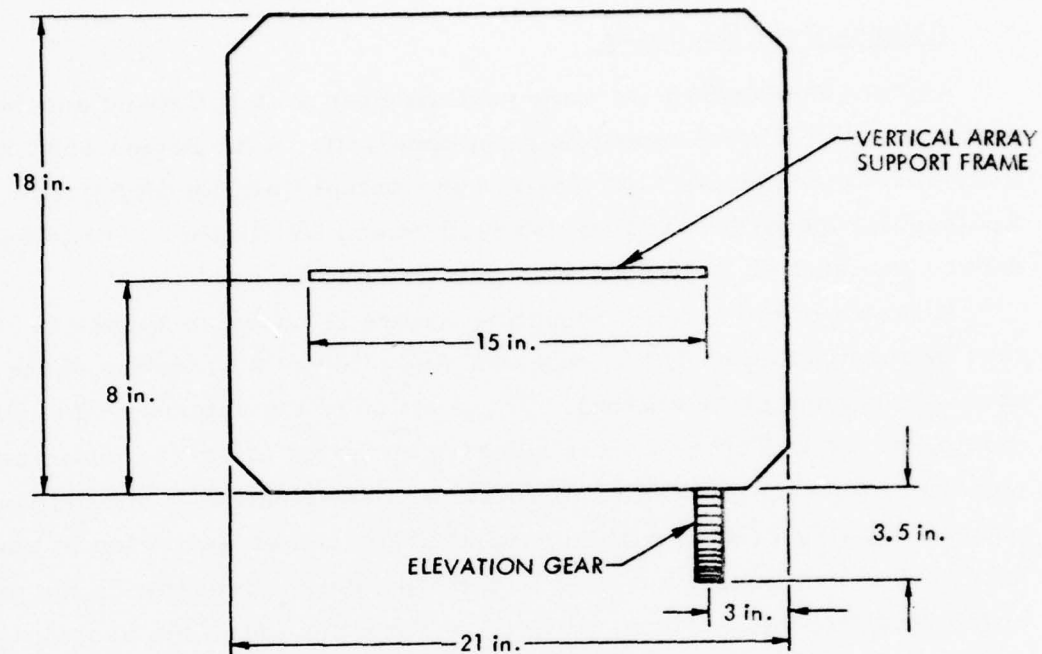


Figure 7 - Plan View of Mounting Fixture on EL/AZ Mount

### 2.3 Band Isolation

Due to the limitations of the available range facility, the capability to simultaneously form independent beams in each frequency band must be inferred from band isolation measurements. These measurements were made for individual half-elements and for fully-excited elements.

In general, the results indicate that significant band isolation (>20 dB) can be achieved at the element using the coaxial-type low frequency notch exciter described in Section 3. However, as described in Subsection 3.2, a resonance notch occurs at 8.0 GHz for the low frequency exciter developed in this program. Consequently, isolation is significantly degraded at 8.0 GHz.



In the array environment, isolation is determined on receive, holding frequency, transmitter power and array aperture fixed. Hence, aperture gain remains constant, and the received power represents true isolation for either transmit or receive provided that in transmit, the two high frequency ports in each half guide are equally excited in amplitude and phase\*.

The band isolation data for broadside incidence is summarized in Table 1. Except at 8 GHz, the isolation, as measured at the top and bottom low frequency ports, shows the exciters are reasonably well balanced in the measurement band. The significant decrease in isolation at 8.00 GHz is due to the previously mentioned resonance which is discussed fully in Section 3. The strong band coupling at 8.64 GHz was anticipated and reflects the limitations of the present low frequency exciter design, although not the concept.

At the high frequency ports, the isolation exceeds 32 dB throughout the 4 GHz design band. This high isolation results from two sources. First, the stripline-fed notch exciter exhibits a low frequency cutoff, similar to that observed for the isolated flared notch stripline antenna<sup>(4, 5)</sup>. For the particular exciter developed for the dual frequency array, this cutoff occurs in the vicinity of 6.0 GHz. Second, fields in the feedguides of the low frequency exciters are evanescent in the 4 GHz band. For the present case, the attenuation is 26.6 dB/in. at 4 GHz rearward of the notch.

---

\* For a  $\delta$  phase difference between high frequency ports within a single frequency, the excitation amplitude of the LSE<sub>10</sub> mode in the GHz band is proportional to  $\cos(\delta/2)$ . Hence, on transmit, the isolation at the low frequency port increases with scan.

TABLE 1  
MEASURED BROADSIDE ISOLATION

Broadside Isolation (dB Below Inband Port)

Measurement Frequency (GHz)	Configuration		
	Top Half Element*	Bottom Half Element*	Fully Excited Element
3.68	-	-	> 36
3.80	-	-	> 36
4.00	-	-	> 37
4.20	-	-	33.5
4.32	-	-	32.0
7.36	22.0	25.8	20
7.60	23.5	26.2	21.5
8.00	31.9	7.4	12.0
8.40	>29.0	23.0	26.0
8.64	10.7	7.5	10.0

\* Half element isolation measurements were not made in the 4 GHz band.

Figure 8 shows fully excited element low frequency port isolation as a function of H-plane scan at four sample frequencies in the 8 GHz band. The high frequency ports are equiphased resulting in broadside scan of the four high frequency phase centers. For this phasing condition, both high and low frequency measurement ports are decoupled from the  $LSE_{20}$  mode, and incidence angle independent isolation should be obtained. The asymmetry at 8 and 8.64 GHz is not fully understood, but occurs only in the low frequency port. One would anticipate similar behavior in the 4 GHz band. However, due to the high isolation achieved, the resulting out-of-band patterns at the high frequency ports were too noisy for valid comparison.

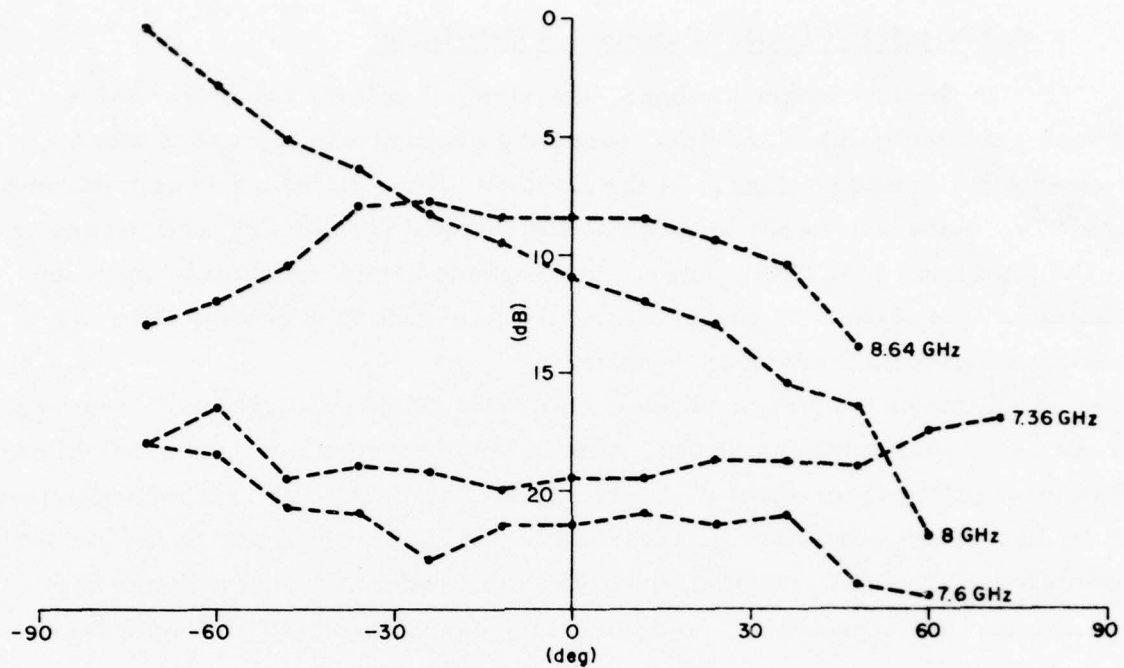


Figure 8 - Measured Isolation at Low Frequency Port - H-Plane Incidence -  $12^\circ$  Sampling Interval

#### 2.4 Central Element Pattern

To ascertain the principal plane scan properties of the dual frequency element, extensive studies of central element pattern were conducted at five sample frequencies in each band, viz,  $\pm 8$  percent,  $\pm 5$  percent and center frequency. In both measurement bands, H-plane element patterns were found to be in excellent agreement with previously predicted realized gain<sup>(2)</sup>. In the E-plane, ground plane edge diffraction produced significant pattern distortion above 3.68 GHz. In the 4 GHz band, the effects could not be eliminated. However, in the 8 GHz band, the edge excitation was reduced by exciting the full element for the broadside scan condition.

### 2.4.1 Central Element Pattern - 4 GHz Band

In the low frequency band, the element pattern characteristics (hence realized gain) of the dual frequency element are typical of more conventional configurations. In the H-plane, the gain falloff is approximately  $\cos^{3/2} \theta$  - being somewhat broader at the low end (3.68 GHz); and narrower at the high end (4.32 GHz), due to the increased field concentration in the vicinity of the slabs. In the E-plane, the gain-fall is narrower than  $\cos \theta$ , and broadens with increasing frequency.

Figures 9 through 11 show comparisons of predicted and measured H-plane element patterns at low, mid and high frequencies in the 4 GHz band. The level of the theoretical curve is adjusted to best fit the measured pattern in an LSS sense. In general, measured element patterns are narrower than predicted. This is due primarily to the interaction of the low frequency exciter and the aperture. The asymmetry has been associated with the

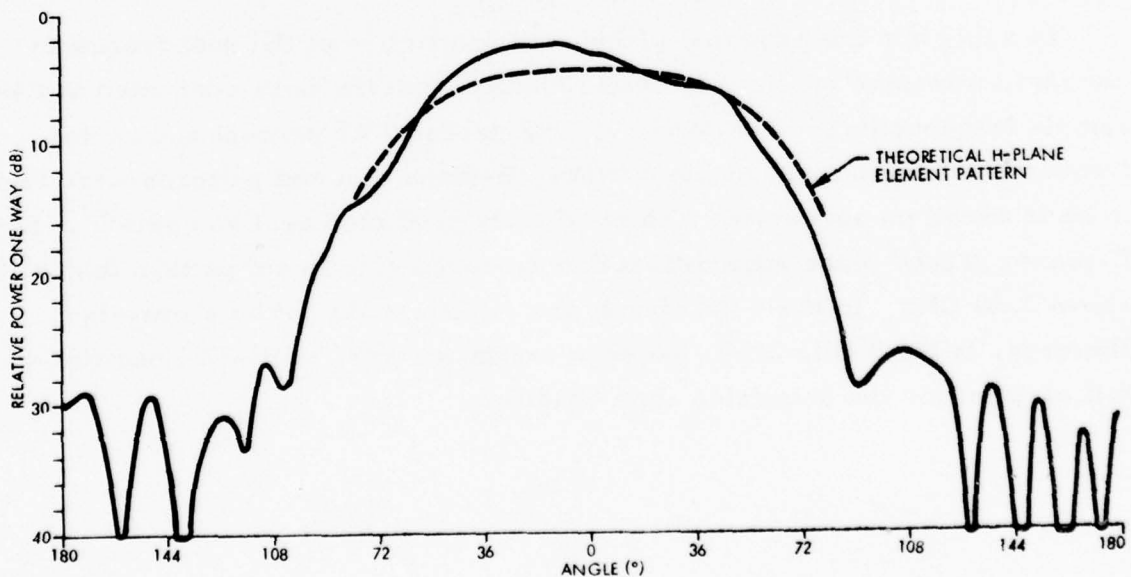


Figure 9 - H-Plane Element Pattern, F = 3.68 GHz

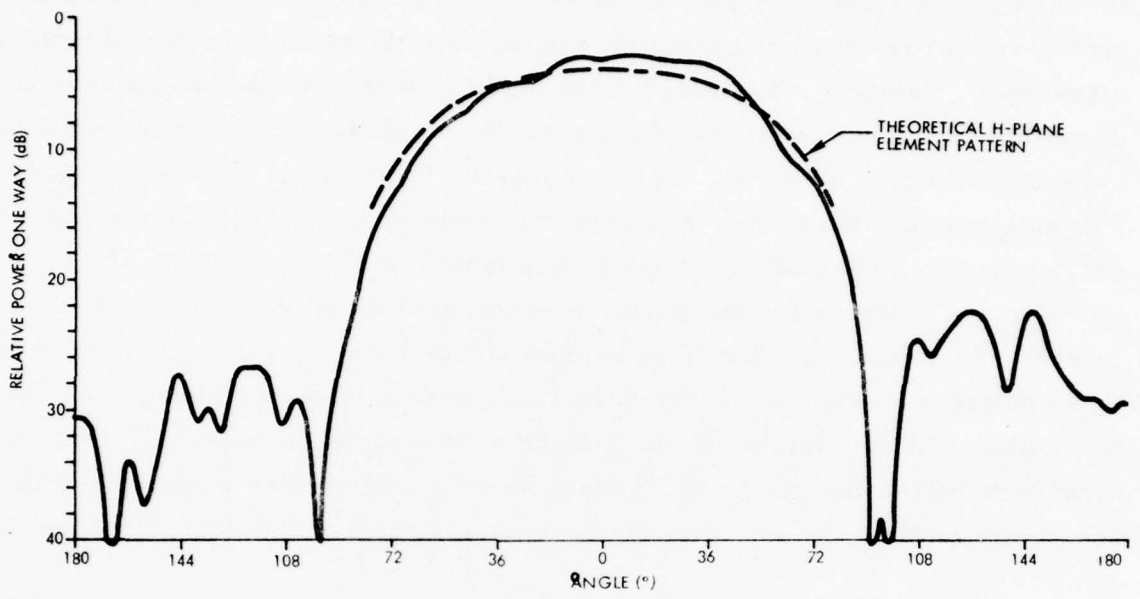


Figure 10 - H-Plane Element Pattern,  $F = 4.00$  GHz

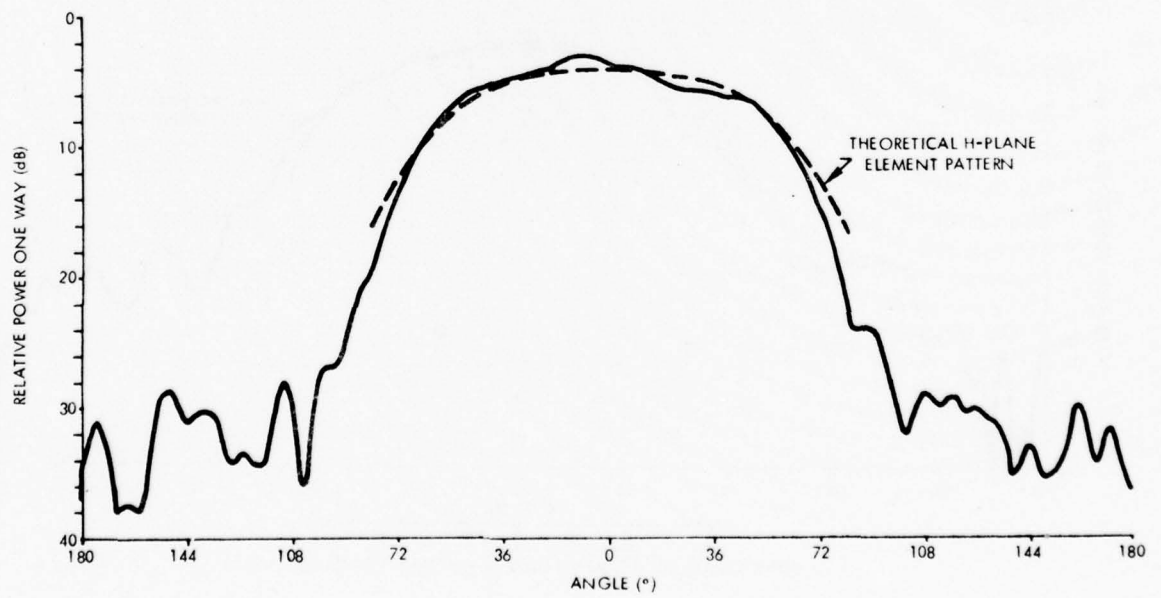


Figure 11 - H-Plane Element Pattern,  $F = 4.32$  GHz



elevation gear on the test mount which protrudes approximately 3.5 in. forward on the right hand side of the table. This gear was identified as a strong scatterer which could not be entirely eliminated for the broad patterns measured. However, it is clear from these measurements that the interaction of the low frequency exciter and the aperture tends to reduce the H-plane scan coverage by 1 to 2 dB at  $60^\circ$  from broadside. This is not atypical of more conventional configurations, and evidently requires a modification of the exciter design such that an off-broadside match is achieved.

E-plane patterns for the center element are shown in Figures 12 through 14 at the low, mid, and high frequencies of the 4 GHz band. It is evident from these patterns that the edge diffraction is a strong influence above 3.68 GHz, particularly in the vicinity of  $36^\circ$ , which corresponds to the outermost, and strongest diffraction peak. The locations of the diffraction peaks and nulls are shown on the figures. The strong asymmetry in the 4 GHz pattern is due

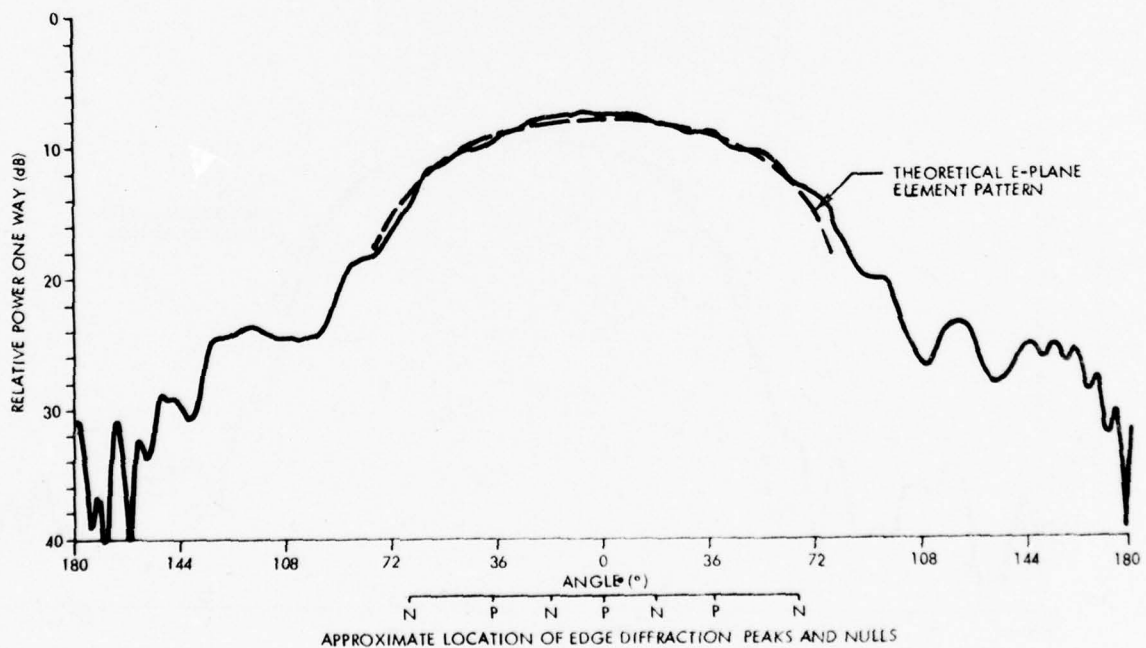


Figure 12 - E-Plane Element Pattern,  $F = 3.68$  GHz

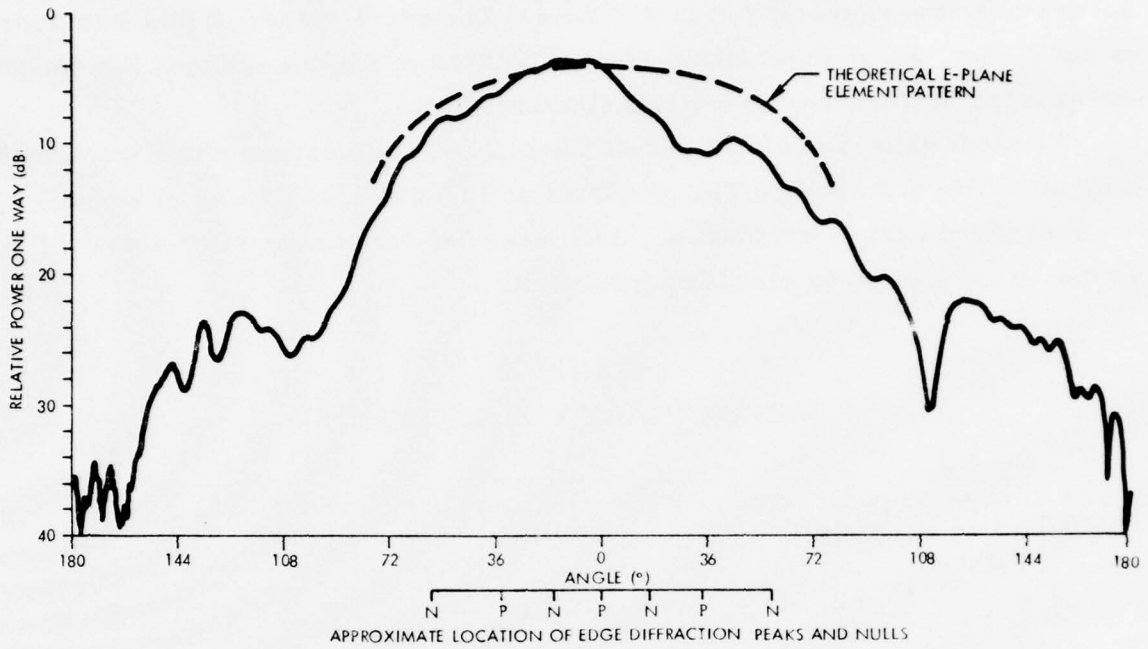


Figure 13 - E-Plane Element Pattern, F = 4.00 GHz

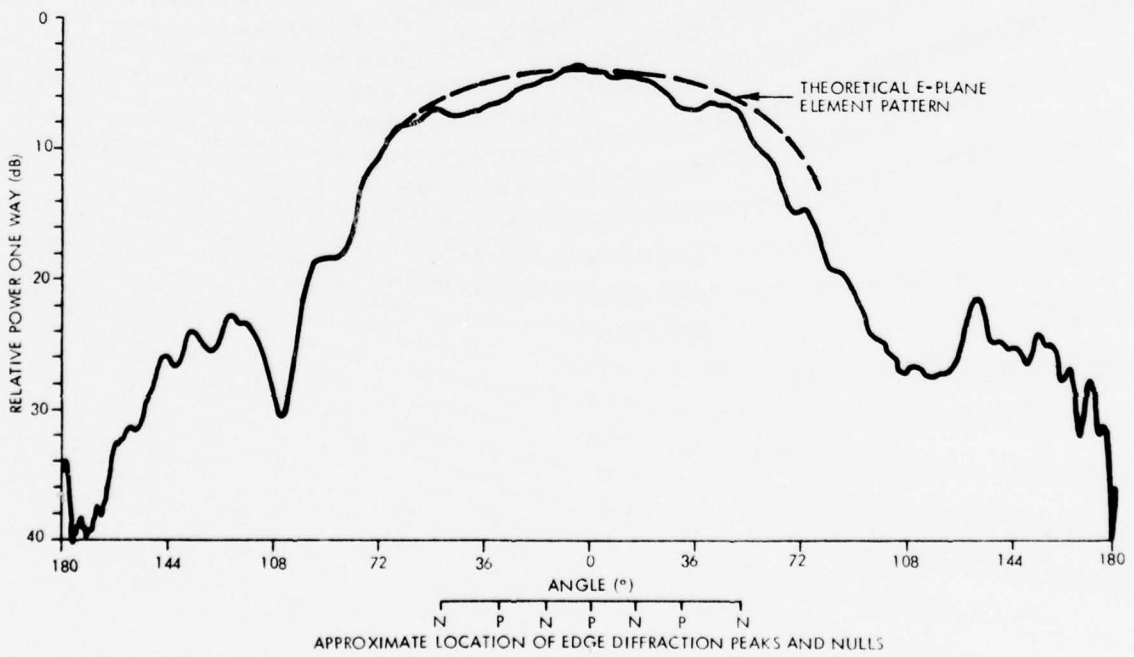


Figure 14 - E-Plane Element Pattern, F = 4.32 GHz

to an imbalance between the upper and lower low frequency exciters and occurs over the range of 3.8 to 4.1 GHz. The exact nature of this imbalance is not known, but is most likely related to exciter location and exciter-to-guide wall contact differences in the two element halves.

Element gain is summarized in Table 2. Gain measurements were made only at 4 GHz and above. The gain loss at 4.2 and 4.36 GHz is in keeping with the measured exciter mismatch. The increase over the area gain at 4 GHz is due to the narrowed elevation beamwidth.

TABLE 2  
GAIN SUMMARY FOR 4 GHz BAND

Frequency (GHz)	Cell Gain (dB)	Reflection Loss (dB)	Measured Gain (dB)	$\Delta$ (dB)
4.0	3.18	0.23	3.50	+0.55
4.2	3.60	0.24	2.90	-0.46
4.32	3.85	0.25	3.30	-0.30

# UNCLASSIFIED

## 2.4.2 Central Element Pattern - 8 GHz Band

For conventional array configurations, the realized gain pattern, i. e.,  $(1 - |\Gamma|^2) \cos \theta$ , is synonymous with the pattern of a near center element (assuming a sufficiently large array). For the twin slab dual frequency element, this identification holds only in the low frequency band. In the high frequency band, gain fall-off with scan is typical of single frequency configurations, as was demonstrated in Reference 2. However, the H-plane pattern associated with each high frequency phase center is asymmetric. This asymmetry is evidently associated with the aperture properties and is influenced by the distance from the effective excitation plane of the twin slab guide to the aperture.

The principal features of this asymmetry are illustrated in Figure 15, which shows a schematic representation of a typical single port receive configuration and resultant pattern. With respect to the array normal, the left-hand frequency port is load terminated and the right-hand port is connected to a receiver. With a plane wave incident from the right, there is an

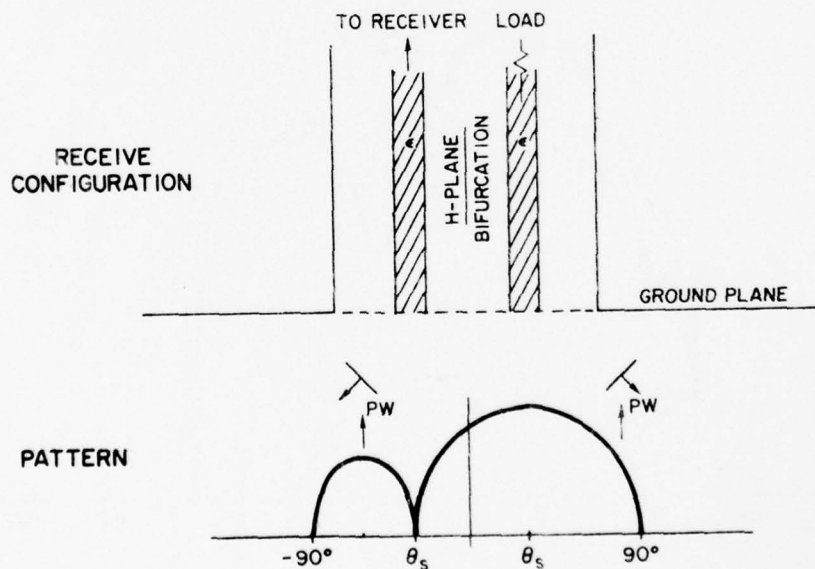


Figure 15 - Schematic Representation of Individual Phase Center H-Plane Pattern

# UNCLASSIFIED

angle,  $\theta_s$ , for which the energy coupled into the twin slab feedguide is predominantly confined to the right-hand slab, and the received signal is maximum. Conversely, for a plane wave incident from the left, at or near  $-\theta_s$ , the energy is primarily confined to the left-hand slab, and the received signal is small.

These general pattern properties are predicted by multimode infinite array theory, as shown in the Appendix. In particular, the "null" indicated in Figure 15 is an early resonance type phenomenon associated with  $(-1, 0)$  and  $(-1, -1)$  grating lobe incipience, and the peak is apparently an antiresonance.

Figure 16 shows a measured individual phase center pattern pair for an isolated twin slab feedguide in a large ground plane. The ground plane is developed on the array by copper taping all but the excited aperture. Pattern features are obtained which are similar to those for the array element, with the distinction that the pattern nulls are approximately  $8^\circ$  closer to broadside than the associated peaks, and the peak to null separation is  $2\pi d(\sin\theta_p - \sin\theta_n)/\lambda = 90^\circ$ , where  $d$  is the center-to-center slab spacing. Since it can be

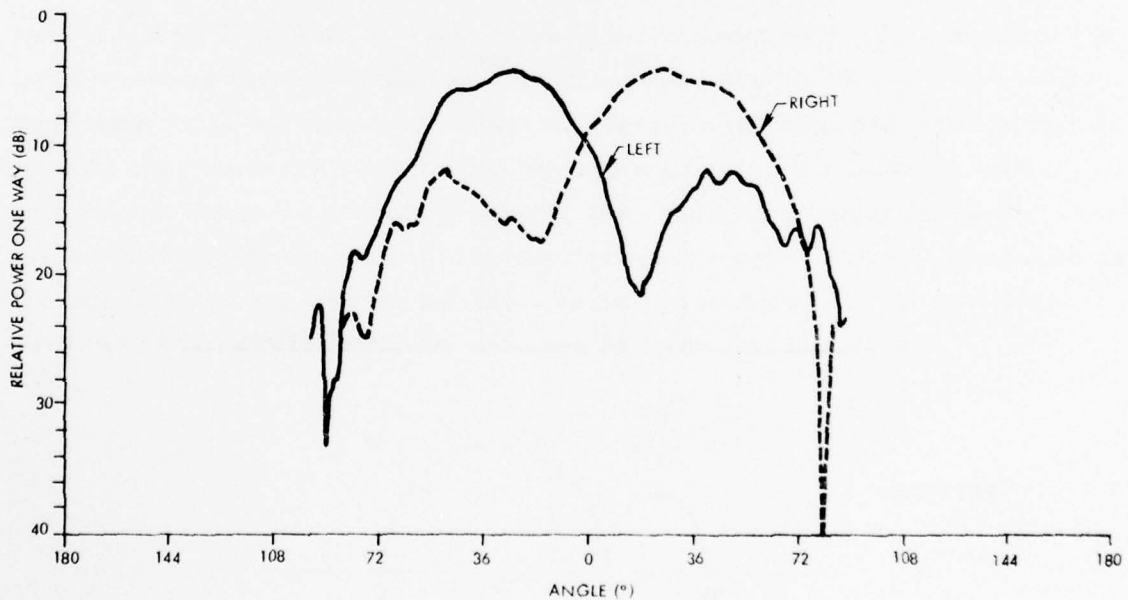


Figure 16 - Individual Phase Center H-Plane Patterns -  
Isolated Dual Frequency Element



## UNCLASSIFIED

demonstrated that there is insufficient phase length in the elements to account for these anomalies, it must be concluded that the relative amplitude and phase weighting of the  $LSE_{10}$  and  $LSE_{20}$  modes differ significantly from what might be expected from simple two mode arguments. Specifically, the complex interactions at the aperture evidently produce opposite phase rotations of the two modal voltages, effectively providing an additional delay for the  $LSE_{10}$  mode and an advance for the  $LSE_{20}$  mode.

The existence of this resonance null has the effect of increasing the gain falloff with scan, as compared with a conventional array. This is immediately evident when one tries to form a beam by superimposing the pairs in Figure 16. At broadside, only the  $LSE_{10}$  mode is coupled to the high frequency exciters, and the pattern is approximately that of two co-phased isotropes separated by the slab center-to-center distance (0.750 in). As the excitation phase of the phase center patterns is altered to produce a scanned beam, the relative pattern amplitude weightings become immediately dissimilar, and one of the pair predominates - hence, the pattern smears out, reducing element gain.

As a side note, the realized gain pattern of the array element is therefore the sum of the individual phase center field patterns, as demonstrated in Figure 17. The data shown is an approximation since only amplitude data is taken in the measurement program. However, it should be intuitively obvious that, since the patterns are generated by the same physical aperture, the direct sum must correspond to array main beam scan loss.

UNCLASSIFIED

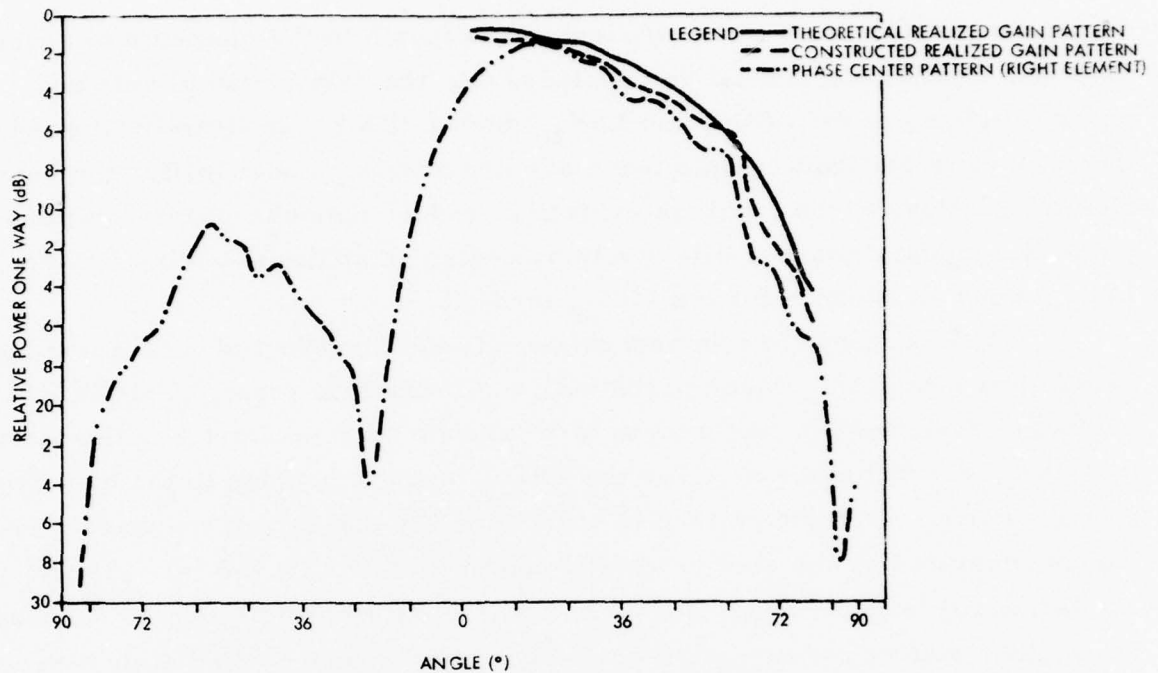


Figure 17 - Constructed H-Plane Element Pattern, F = 8 GHz

Figures 18 through 22 show phase center patterns for the top element half at 7.36, 7.6, 8.0, 8.4 and 8.64 GHz, respectively. In general these patterns show the principal features discussed above. As is discussed in Appendix, it is not possible, with the current analytical model to accurately predict the phase center patterns beyond specifying the location of the peaks and nulls. It can be stated, however, that the null depth is evidently associated with the distance from the low frequency probe notch termination to the aperture plane. From the discussion in the Appendix, it is evident that broader scan coverage can be obtained by reducing this length.

UNCLASSIFIED

UNCLASSIFIED

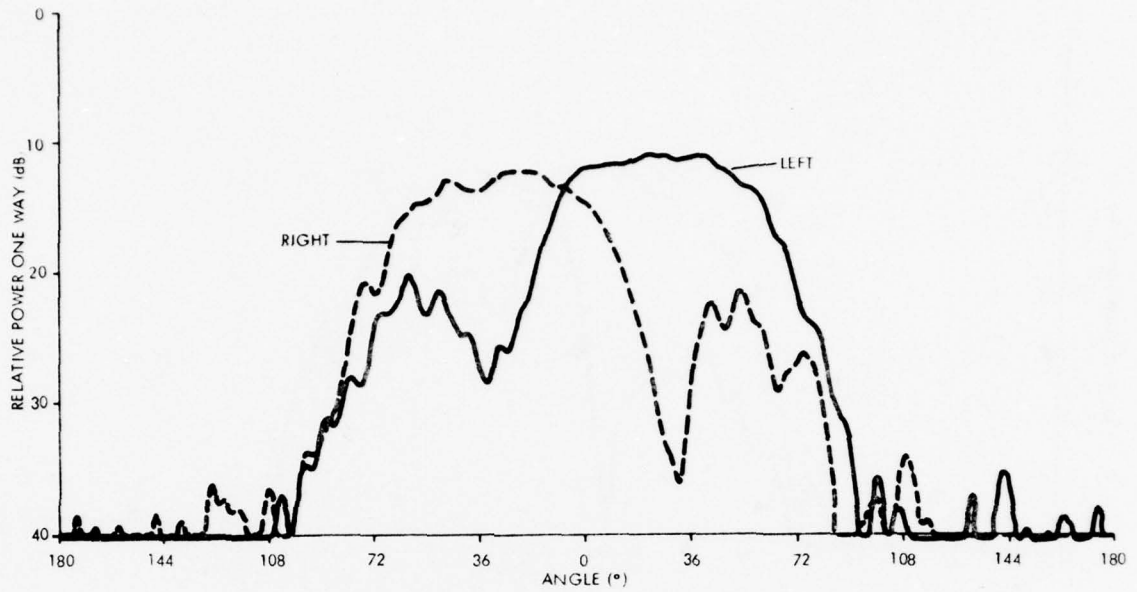


Figure 18 - Individual Phase Center H-Plane Patterns,  $F = 7.36$  GHz

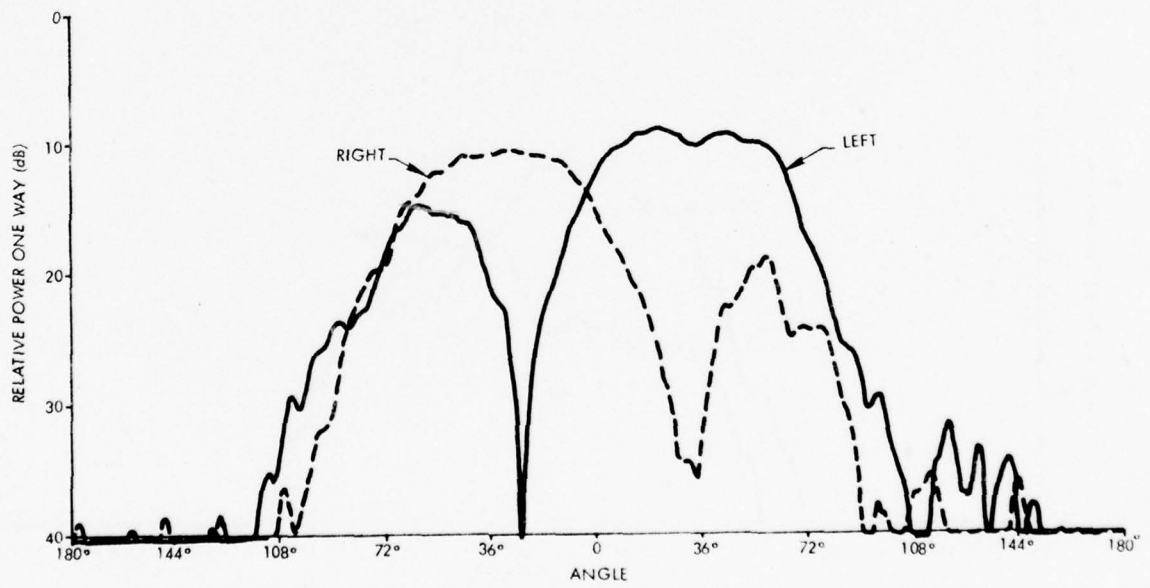


Figure 19 - Individual Phase Center H-Plane Patterns,  $F = 7.60$  GHz

UNCLASSIFIED

UNCLASSIFIED

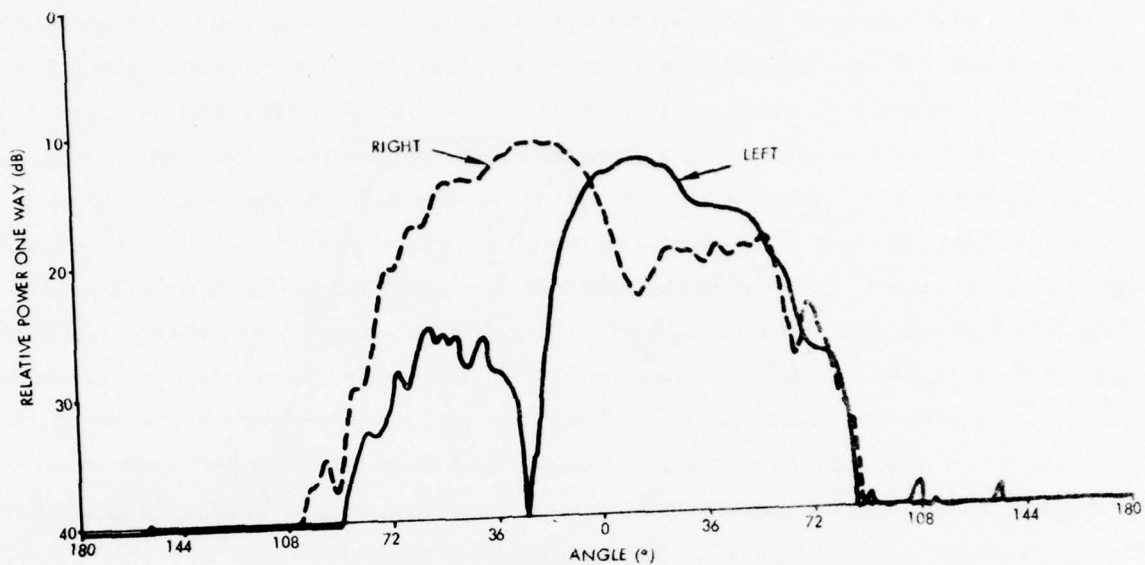


Figure 20 - Individual Phase Center H-Plane Patterns,  $F = 8.00$  GHz

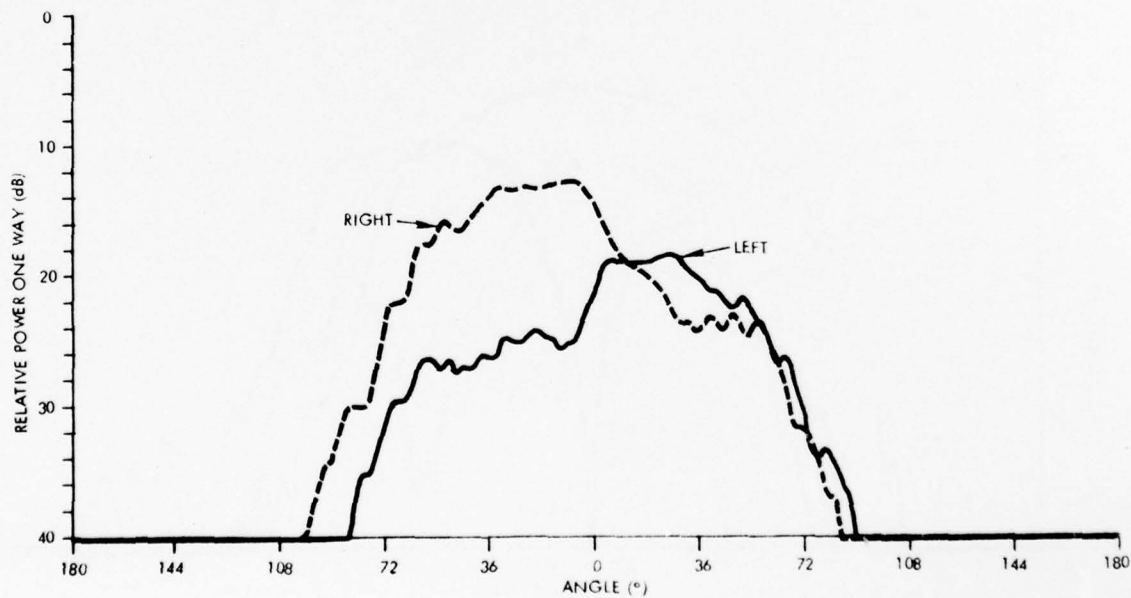


Figure 21 - Individual Phase Center H-Plane Patterns,  $F = 8.40$  GHz

UNCLASSIFIED

UNCLASSIFIED

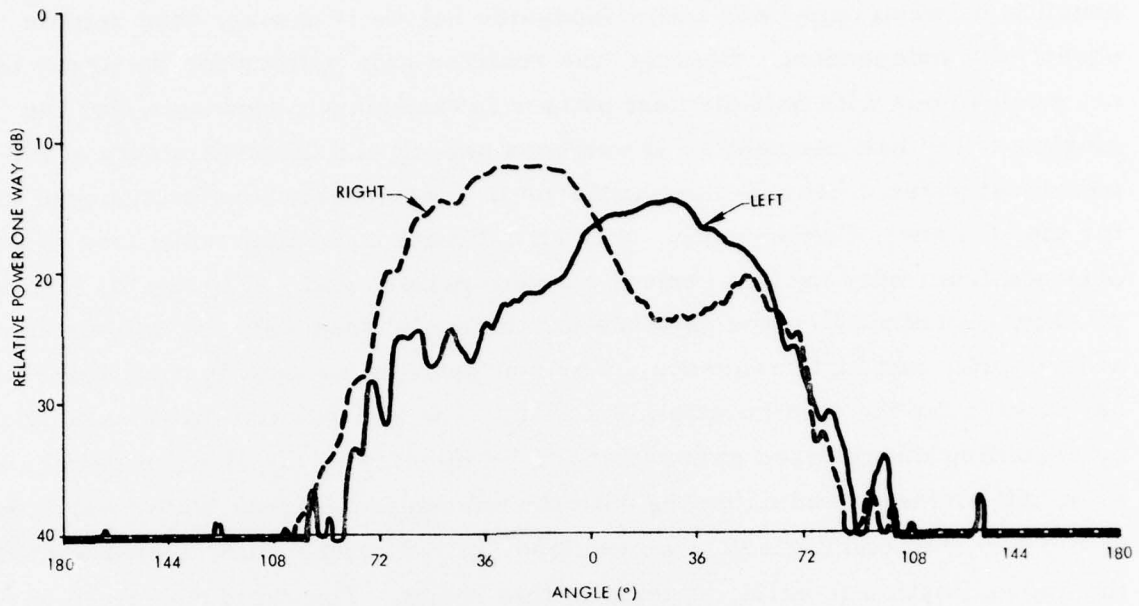


Figure 22 - Individual Phase Center H-Plane Patterns, F = 8.64 GHz

Table 3 summarizes high frequency element gain results. At 8 GHz and below, the discrepancy between measured element gain and theoretical cell gain is consistent with the interaction of two 2:1 mismatches (the high frequency exciter and the aperture). No adequate explanation of gain loss at the higher frequencies has been found.

TABLE 3  
HIGH FREQUENCY GAIN SUMMARY

Frequency (GHz)	Theoretical Element Gain (dB)	Measured Gain (dB)	$\delta$ (dB)
7.36	7.97	7.0	-0.97
7.60	8.25	6.7	-1.55
8.00	8.69	7.2	-1.49
8.40	9.12	5.5	-3.62
8.64	9.39	5.7	-3.69



## UNCLASSIFIED

Similar arguments apply only in part for the E-plane. Although the coupling between upper and lower feedguide halves is strong, they remain essentially independent. Clearly, the realized gain pattern for the array is not synonymous with half element pattern in this plane. However, for the singly excited half element no resonances occur, and the asymmetry of the individual phase center E-plane patterns is considerably less pronounced than for the H-plane. Consequently, only an estimate of E-plane scan loss can be obtained from fully excited central element pattern data. Figures 23 through 25 show measured E-plane patterns for the equiphased fully excited element at low, mid, and high frequency. For comparison, an approximate theoretical pattern for the configuration is shown. The approximate pattern is obtained by assuming the realized gain pattern to be identically the element pattern for each half element, and summing with the conventional array factor weighting. Out to  $60^\circ$ , the comparison is quite close, at 7.36 and 8 GHz, indicating that the approximation is valid, at least in this range. The rapid departure beyond  $60^\circ$  may be due either to excessive edge contribution, or factors invalidating the approximation. No explanation has been found for the result at 8.64 GHz.

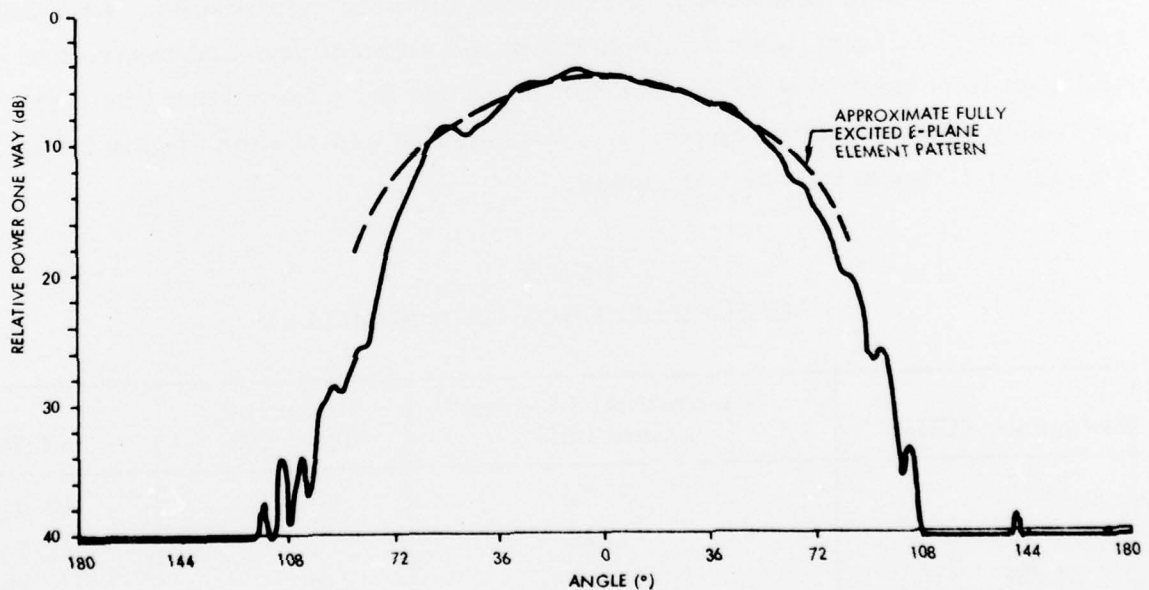


Figure 23 - E-Plane Pattern at Fully Excited Element,  $F = 7.36$  GHz

UNCLASSIFIED

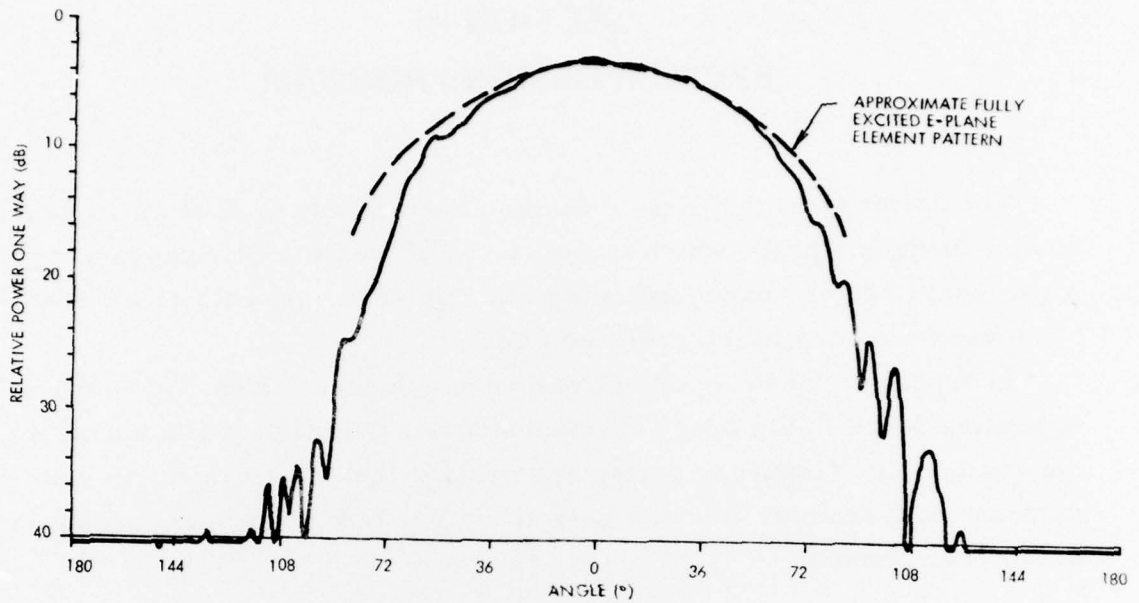


Figure 24 - E-Plane Pattern at Fully Excited Element,  $F = 8.00$  GHz

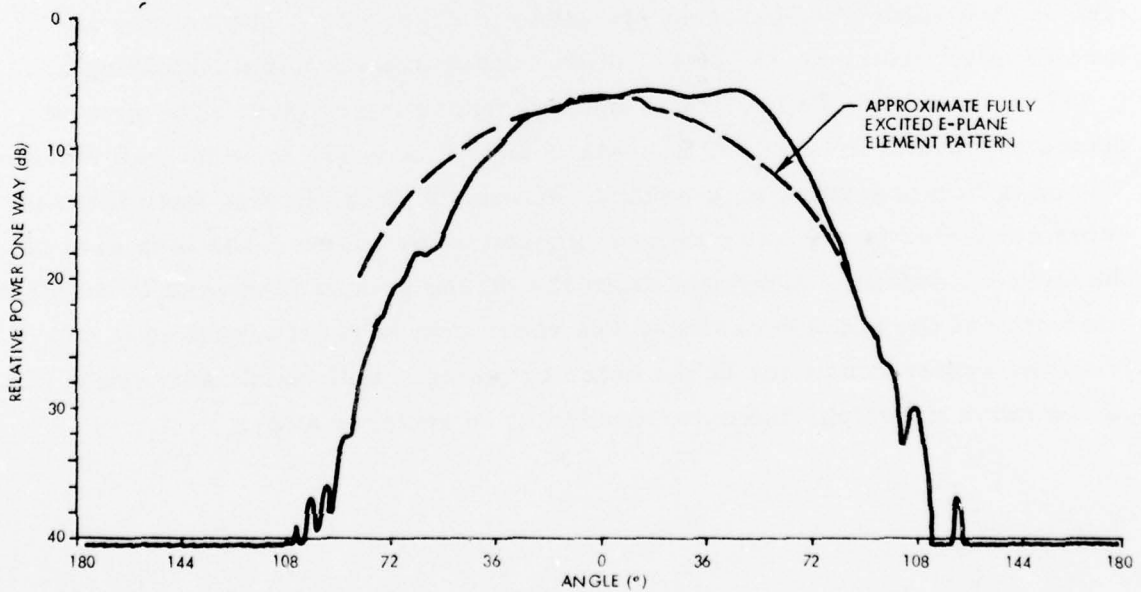


Figure 25 - E-Plane Pattern of Fully Excited Element,  $F = 8.64$  GHz

UNCLASSIFIED

## SECTION III

### EXCITER DESIGN PROGRAM

The objective of the exciter design program was to develop a low frequency feedguide probe which is well matched in the 4 GHz band, and provide significant (> 20 dB) band isolation at the element. An exciter for the 8 GHz band was developed in the previous effort.

In essence, the above objectives were achieved. Measured band isolation exceeding 30 dB in the array environment was demonstrated over the 4 GHz band at the high frequency ports, and greater than 20 dB isolation was demonstrated from 7.36 to 8.4 GHz at the low frequency ports, again in the array environment.

#### 3.1 Low Frequency Exciter - Description

A schematic representation of the feedguide interface to the low and high frequency exciters was shown in Figure 2. The details of the low frequency exciter configuration are given in Figure 26. The exciter is formed of two notched, 0.020 in. thick copper ground planes shielding a 0.047 in. diameter Teflon loaded coaxial transmission line. The ground planes are 0.400 in. x 2.255 in. with 0.100 in. x 1.175 in. centered notches. The coax line is formed as a squared format "J" and situated such that the outer conductor is coplanar with the ground plane edges. The long arm of the "J" is 1.455 in., measured from the closed ground plane end to the center conductor at the notch crossing. The short arm is short circuited 0.650 in. from the center conductor at the notch crossing. Both bend radii are 0.050 in. At the notch crossing, the outer conductor is stripped away.

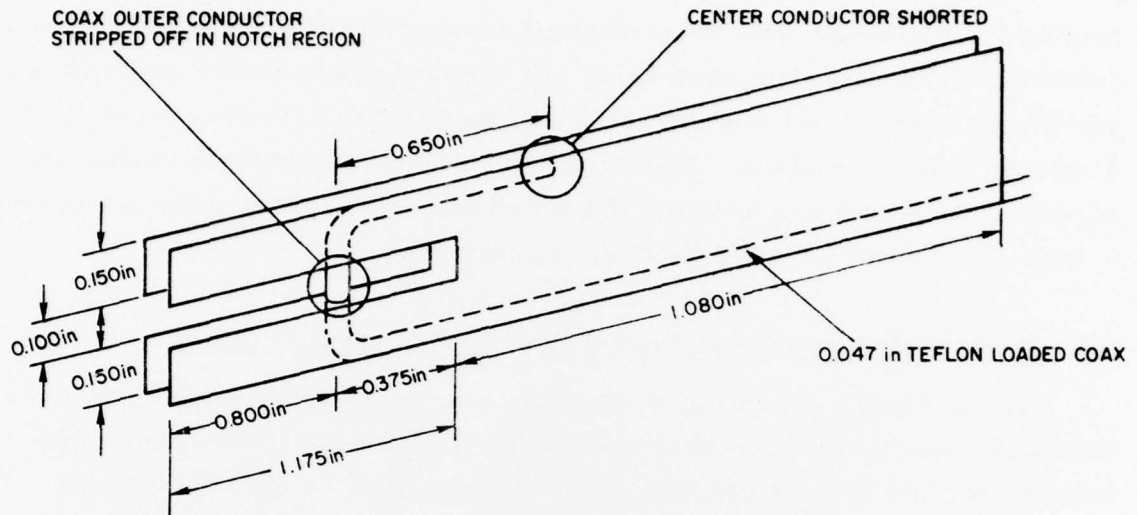


Figure 26 - Coax Fed Notch Exciter

With the exciter inserted in the twin slab feedguide, the notch region is characteristic of an inhomogeneously loaded double ridged guide. For the small notch width, the low frequency band fields are concentrated in the notch, and the longitudinal wavenumber of the dominant mode approaches that of free space. In the high frequency band, however, the notch region fields are concentrated primarily in the dielectric slabs: the odd mode wavenumber is essentially that for the twin slab region, and the even mode wavenumber approaches that for the odd mode as the notch is closed. Hence, the introduction of the notch in the feedguide has the desirable feature of reducing the phase error due to unequal dispersion of the two modes.

Basically, the coax-to-notch region transition is a four port network. The two coax ports are terminated with a generator (or load) and short circuit. The notch region ports are terminated by the notch bottom and inhomogeneously loaded ridge guide to double slab (forward) discontinuity. In the high frequency band, the notch bottom and forward discontinuities have small capacitive susceptances typical of a thick wall H-plane bifurcation in the twin



slab guide, which at 8 GHz has a VSWR less than 1.1 for a 0.068 in. wall.\* Hence, in this band, the rejection characteristics of the exciter are governed primarily by the distance to the coax short circuit, which behaves as a top loading for the probe; and the scattering characteristics of the notch-to-coax junction. In the low frequency band, the forward discontinuity presents a more significant susceptance and the notch bottom appears as a short circuit at a displaced reference plane. Consequently, a match is obtained in this band by adjusting the length and height of the notch and the location of the probe within it for a fixed notch-to-coax short circuit distance.

### 3.2 Exciter Performance in Load Terminated Twin Slab Guide

Exciter design and initial evaluation were performed in load terminated twin slab feedguide. To ensure that higher order modes were reactively terminated, the test fixture was 7.300 in. long ( $\sim 2\lambda_g$  at 4 GHz). The loading consisted of five 1.7 in. tapered  $300\ \Omega$  card loads. One load was centered in the cross-section, the remaining four were bonded to the slabs on either side.

Figure 27 shows exciter reflection coefficient magnitude from 3.0 to 9.0 GHz, for the final prototype exciter in the twin slab feedguide. In the design band, 3.68 to 4.32 GHz, the reflection coefficient is below 0.3. From 4.32 GHz to approximately 4.7 GHz,  $|\Gamma|$  increases rapidly with frequency, then remains flat to 6 GHz. In the 4.7 to 6 GHz region the  $LSE_{10}$  mode of the single slab feedguide passes from evanescent to propagating and the reflection phase of the notch bottom remains relatively linear with frequency. Above 6 GHz the influence of the coax short circuit dominates, and  $|\Gamma|$  becomes unity at 7.65 GHz as would be anticipated from the arguments in Subsection 3.1 (for a probe that is not resonant at this frequency).

---

\* A complete analytical description of coax and stripline fed exciter types has not been developed. Certain, simple discontinuities have been analyzed for the twin slab feedguide in order to better understand the exciter properties. The VSWR given here is computed from a multimode model for thick wall H-plane bifurcation scattering.



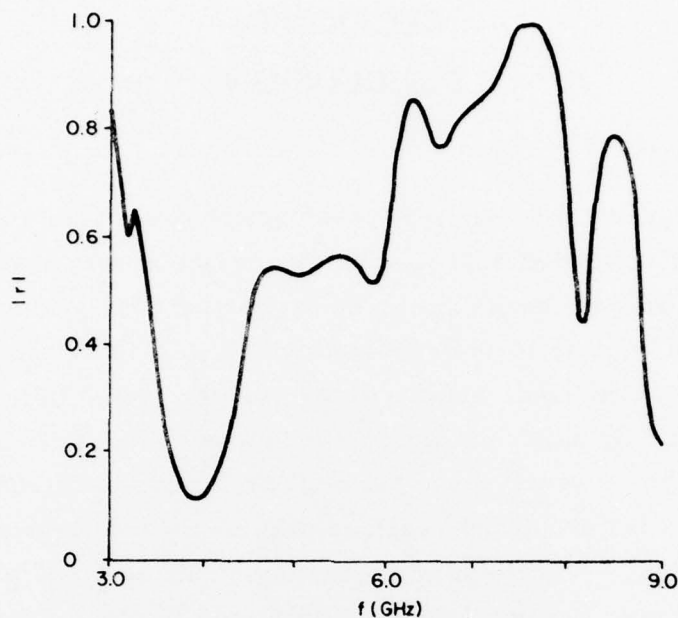


Figure 27 - Reflection Coefficient Magnitude for Coax Fed Exciter

At 8 GHz, a transmission resonance type behavior is exhibited by the exciter, which is characteristic of a heavily loaded short dipole (monopole) probe. The primary influence on the location and depth of the resonance is the height of the notch. Smaller notch heights tend to move the resonance to higher frequency; and, for the range of notches studied, tend to increase the coupling to the  $LSE_{10}$  mode at the high frequency resonance, and decrease the coupling in the design band. The notch height for the array measurement program was selected to minimize reflection loss in the 4 GHz band in spite of the resonance at the center of the high frequency band.

As a consequence of the resonance behavior in the 8 GHz band, probe and notch alignment are critical for the coax-fed notch exciter. Small errors in the length of exposed center conductor introduce additional susceptances at the probe to coax transitions, altering the high frequency resonant behavior and low frequency match. These characteristics are evident for the two exciters fabricated for the array measurement phase. The exciter for the top element half had slightly skewed ground planes resulting in an effective reduction of the notch height of approximately 0.020 in., and an increase in the resonant frequency. This explains the high isolation achieved in this half at 8 GHz.

## SECTION IV CONCLUSIONS

Previously predicted principal plane scan properties of the bifurcated twin dielectric slab loaded dual frequency array element have been demonstrated over 16 percent bands centered at 4 and 8 GHz; and a novel feedguide mode launcher has been developed which is matched to better than 2:1 over the entire 4 GHz band, and provides greater than 20 dB isolation over portions of the 8 GHz band. In the low frequency band, measured central element pattern in a twenty-three element array has been shown to be in good agreement with predicted realized gain in E- and H-planes from broadside to 60° incidence. In the high frequency band, H-plane phase center patterns correlated with realized element gain; and E-plane fully excited element patterns are shown to be in good agreement with predicted patterns.

The 4 GHz band feedguide mode launcher developed is a coax-fed notch type exciter. Investigations of the exciter in array and load terminated feedguide environments have demonstrated:

- Significant band isolation (> 20 dB) can be achieved at the element level.
- Better than 2:1 exciter match can be achieved in load terminated twin slab feedguide over the entire 4 GHz band.
- High Q passbands in the 8 GHz band can be eliminated by narrowing the notch height.

The presence of the high Q passbands in the 8 GHz band is not seen to be a fundamental limitation of the device, but this does constitute an area where additional development could bring about improved performance.

## SECTION V

### REFERENCES

- 1) Mailloux, R. J., "Dual Band Phased Array Elements", U. S. Pat. No. 3882505, 6 May 1975.
- 2) Pozgay, J. H., Fassett, M., and Lewis, L. R., "Design and Analysis of Bifurcated Twin Dielectric Slab Loaded Rectangular Waveguide Dual Frequency Array Elements", Final Report RADC-TR-77-160, April 1977.
- 3) Lewis, L. R., Fassett, M., and Hunt, C. J., "A Broadband Stripline Array Element", IEEE/AP-S Symposium, June 1974, Atlanta, GA.
- 4) Lewis, L. R., Pozgay, J. H., and Hessel, A., "Design and Analysis of Broadband Notch Antennas and Arrays", IEEE/AP-S International Symposium, October 1976, Amherst, MA.
- 5) Lewis, L. R. and Pozgay, J. H., "Broadband Antenna Study", Final Report AFCRL-TR-0178, March 1975.

# UNCLASSIFIED

## APPENDIX A HIGH FREQUENCY PHASE CENTER PATTERNS

As described in Section 2.4.2, the apparent high frequency phase centers in a single twin slab guide are strongly coupled, producing asymmetric patterns for excitation of the individual high frequency ports. This is evidently due to a significant alteration of  $LSE_{10}$  and  $LSE_{20}$  total modal voltage phases at the aperture. The detailed shape of the patterns is also dependent on the separation of aperture plane and the plane of twin slabguide mode excitation.

As an heuristic example, consider the superposition of two point sources with the specific weightings  $1+d$  and  $1-d$ , where an even excitation is normalized to unity and an odd excitation has complex amplitude  $d$ . The far field is then

$$E(\theta) = 2 \cos(2\pi S \sin \theta) + 2jd \sin(2\pi s \sin \theta) \quad (A-1)$$

where  $s$  is in wavelengths. If  $d$  is taken as  $\exp(j\phi)$ , then

$$|E(\theta)|^2 = 4(1 - \sin \phi \sin 2t) \quad (A-2)$$

where  $t = 2\pi \sin \theta$ . Except for  $\phi = 0$ , the field has a minimum at  $t = 45^\circ$  and maximum at  $t = -45^\circ$ . The locations of the minimum and maximum are clearly independent of  $\phi$ . Clearly, for  $d = |d| \exp(j\phi)$ , the location of the min and max are dependent on the amplitude and are not symmetrically disposed about  $\theta = 0$ . In Equation (A-2), the "null" depth is controlled entirely by the phase of  $d$ . Independent of the amplitude and phase of  $d$ , the "null" and peak are always separated by  $\Delta t = 90^\circ$ .

This simple model provides an interpretation of the measured high frequency phase center patterns. In the isolated and array configurations excitation of a single high frequency exciter produces nearly equal excitation of the  $LSE_{10}$  and  $LSE_{20}$  modes at the termination of the H-plane bifurcation. At this plane the modal fields are approximately in phase. As the excitation plane recedes from the aperture, the depth of the null is increased, and its location stays put, except in the instance that  $|d|$  is significantly larger than unity.



## UNCLASSIFIED

Consequently, the deep nulls observed at 8 GHz and below are evidently associated with phase lengths of the order of  $\phi > 30^\circ$ , which is typical of the separation between the aperture and the low frequency exciter center conductor.

Figure A-1 shows computed infinite array phase center patterns at 8 GHz for two locations of the excitation plane. With the plane taken coincident with the aperture, peak to null depth is 4.64 dB, corresponding to an effective phase advance of the  $LSE_{20}$  mode of approximately  $30^\circ$ . With an added phase lengths of 1.89 in. ( $\phi = 46^\circ$ ), the peak to null ratio is 14.25 dB - the simple theory of equation (A-2) predicts 17.6 dB. As expected, the null does not shift.

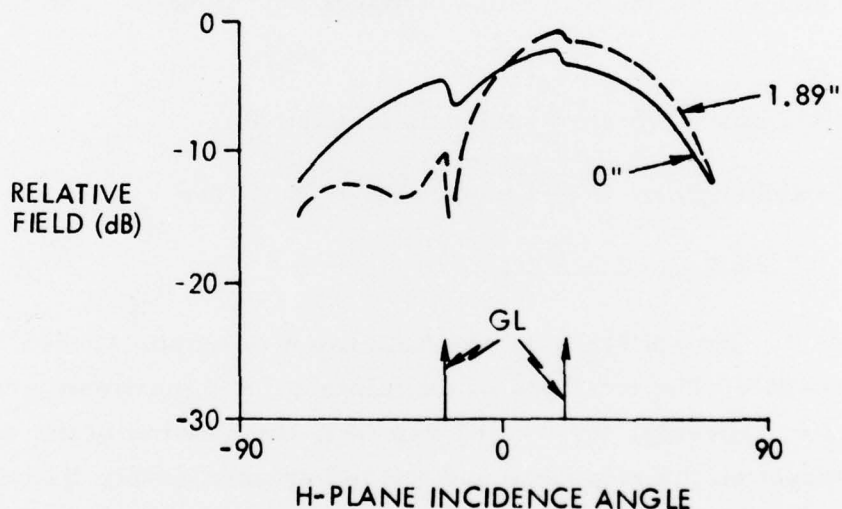


Figure A-1 - Infinite Array Phase Center Patterns at 8 GHz Parameter-Excitation Plane Location

Figure A-2 shows computed infinite array phase center patterns at 7.36 and 8.64 GHz for an added phase length of 0.945 in. The fill in of the null is exactly as expected due to the decrease in dispersion at the higher frequency.



UNCLASSIFIED

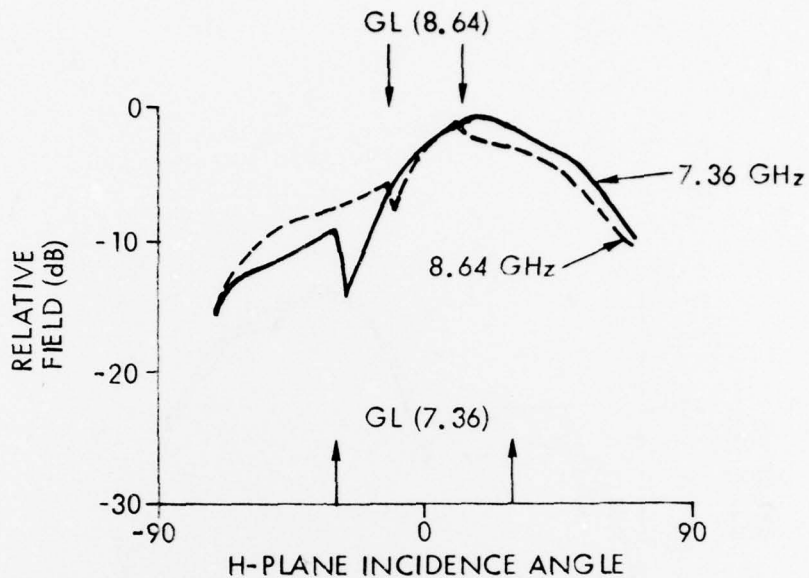


Figure A-2 - Infinite Array Phase Center Patterns - Parameter Frequency - Excitation Plane 0.945 in. Behind Aperture

Unlike the isolated elements, the location of the infinite array pattern null corresponds exactly to the location of the peak. The occurrence just prior to grating lobe incipience warrants classifying these phenomena as early resonances and anti-resonances. To some extent the resonance behavior of the aperture may be eliminated by providing phase delay to the  $LSE_{20}$  mode, which simultaneously has the desirable effects of broadening the scan coverage and, as discussed in reference 2, reducing grating lobe excitation. However, this cannot be readily accomplished with the current exciter configuration. It should be noted that in the instance that the resonance phenomena were eliminated, no H-plane or intercardinal plane grating lobes would be excited since the twin slab element would degenerate to a scanning subarray with null planes containing the spurious beams.

Figure A-3 shows predicted and measured relative phase center patterns at 8 GHz. For comparison a compensation length of 1.89 in. is selected. The good agreement between measured and predicted patterns indicates that the anticipated effective decrease in twin slabguide dispersion in the notch region of the low frequency exciter is not significant.

UNCLASSIFIED

UNCLASSIFIED

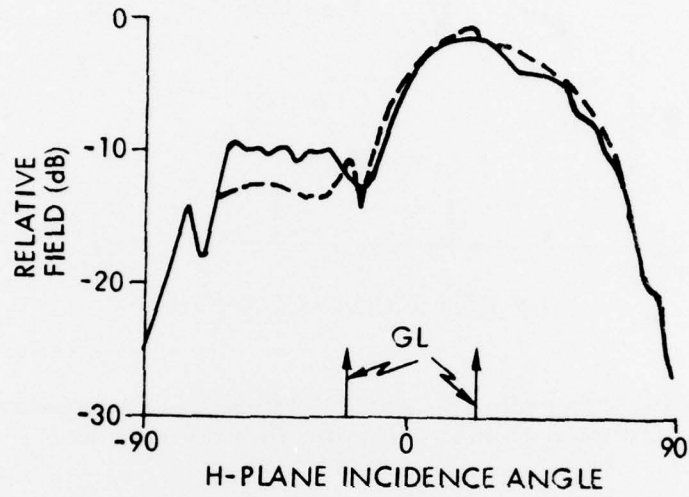


Figure A-3 - Predicted and Measured Relative Phase Center Patterns at 8 GHz - Phase Length of 1.89 in. Assumed

UNCLASSIFIED



*MISSION*  
*of*  
*Rome Air Development Center*

*RADC plans and conducts research, exploratory and advanced development programs in command, control, and communications (C<sup>3</sup>) activities, and in the C<sup>3</sup> areas of information sciences and intelligence. The principal technical mission areas are communications, electromagnetic guidance and control, surveillance of ground and aerospace objects, intelligence data collection and handling, information system technology, ionospheric propagation, solid state sciences, microwave physics and electronic reliability, maintainability and compatibility.*

Printed by  
United States Air Force  
Hanscom AFB, Mass. 01731